ACS OMEGA

Open Access

This article is licensed under CC-BY-NC-ND 4.0

http://pubs.acs.org/journal/acsodf

Article

Catalytic Application of Biochar Functionalized Copper-L-histidine for the Chemo and Homoselective Conversion of Cyanides to Amides and Reduction of Nitroarenes to anilines

Mahrokh Farrokh, Maryam Hajjami,* Mohammad Ali Zolfigol,* and Sepideh Jalali-Mola

Cite This: *ACS Omega* 2024, 9, 47811−47821

Read Online

ACCESS | Metrics & More | Article Recommendations | Supporting Information

ABSTRACT: In our study, we aimed to use olive pomace, food industry waste, as biomass to produce biochar nanoparticles. The surface of the biochar was functionalized with the L-histidine ligand, and then cupric acetate was added to prepare Cu-L-histidine@ biochar as a final catalyst for the chemo- and homoselective synthesis of amide and aniline derivatives. To characterize the novel catalyst, we employed various techniques. Another notable feature of this catalyst is its reusability, which maintained significant efficiency even after multiple uses in reactions.

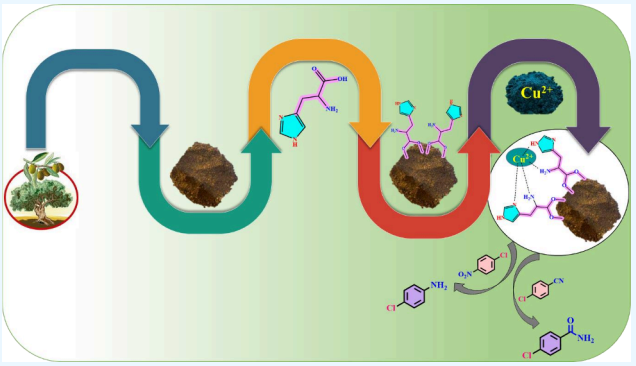

1. INTRODUCTION

Utilization of catalysts in various areas is of great importance. The use of small amounts with high activities is widely desirable for chemical technology and the degradation of environmental pollutants. One possible protocol is the application of metal supported catalysts. Carbon has long been supposed to be a suitable catalyst support material because of its various porous structures, low cost, easy accessibility, good recycling characteristics, compatibility with synthesis variants and wide range of carbonization methods.[1] Biochar nanoparticles are one of the newest supports for the immobilization of organic moieties. They are a class of porous materials which are gained from the pyrolysis of renewable resources and from biomasses under limited oxygen conditions.[2−5] In recent years widespread nano-biochar properties such as catalysis, agriculture and carbon capture applications have been noticed.[6] In fact, biochar is a solid rich in carbon elements, so for the management of agro-food industrial waste, it is suitable to convert it to biochar as a biosorbent for soil and water treatment.[2,7] The surface of biochar is rich in functional groups, which gives it many properties.[8] Also, the source of biochar determines its physiochemical nature. Use of acids, alkali, oxidizing agents and metal ions modification upgrades biochar's attributes.[9]

Amino acids are one of the basic organic materials in the structure of proteins and form about 20% of the human body. They belong to one of these two branches: essential or nonessential amino acids. This class of compounds contains two functional groups, amine and carboxyl groups, which are the center of chemical reactions.[10] The presence of two functional groups gives amphoteric properties to amino acids. One of their significant applications can refer to their catalytic properties, which puts them in the class of green catalysts.[11] In some cases, amino acids and their salts have been used as solvents and absorbents, and their properties related to these functions are owed to their functional groups.[12]

Reduction of the nitro group to amines and anilines is one of the basic reactions which is commonly used in organic synthesis, the pharmaceutical industry, explosives, and fertilizers. This series of reactions can be performed by different methods, for example catalytic reduction in the presence of iron and hydrochloric acid, the Bechamp method, Au/TiO_2, graphene and GO, $Ag/\gamma\text{-}Al_2O_3$ or $Ni/\gamma\text{-}Al_2O_3$; often typical procedures for reduction of the nitro group are less harsh.[13,14,4−6] The reduction of aromatic nitro compounds with noble metal-based catalysts (Pd, Ru, Pt, etc.) is expensive and not cost-effective.[15] Cyanide has wide utilization in large scale industrial processes such as textiles, pharmaceuticals, and mining, especially in gold extraction. So, because of its high toxicity, cyanide is considered a priority pollutant by environmental protection agencies.[16,17] At present, the main treatment idea is to convert cyanide into nontoxic or less toxic

Received: September 14, 2024
Revised: October 27, 2024
Accepted: November 7, 2024
Published: November 19, 2024

© 2024 The Authors. Published by American Chemical Society

Scheme 1. The Stepwise Synthesis of Cu-L-Histidine@biochar

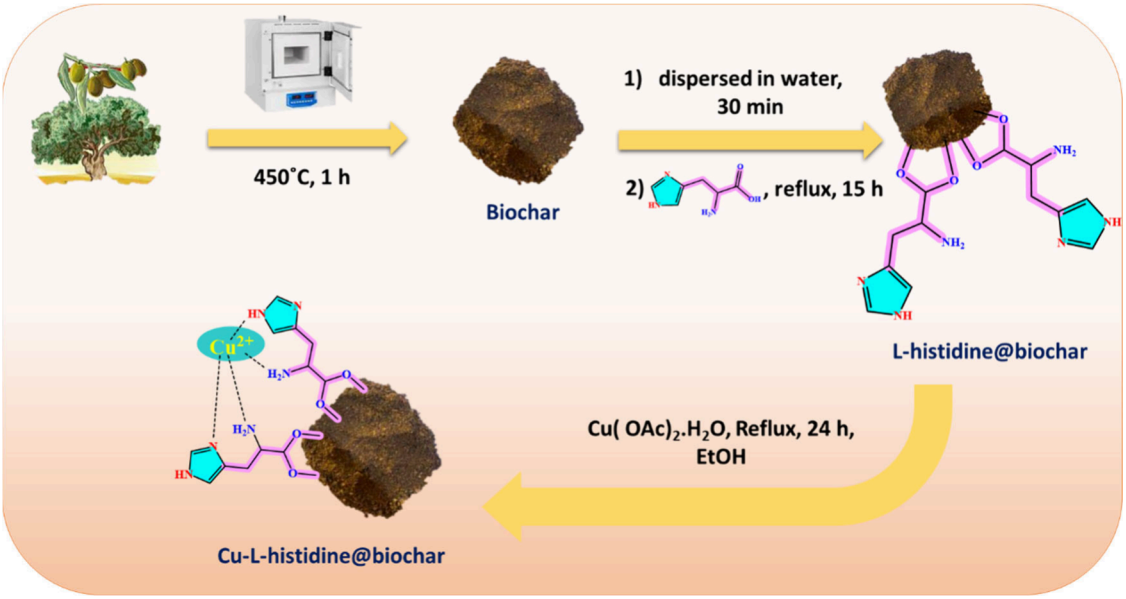

cyanate (CNO-) in wastewater from the gold industry or further convert it to other products such as amides.[17] In this way some different methods have been used, for example electrochemical technologies, $CuxCo_3-xO_4$ electrodes, photocatalytic oxidation, $Bi_4Ti_3O_{12}$, magnetic Ag_3PO_4/RGO/$CoFe_2O_4$, and 3D network structure graph hydrogel-Fe_3O_4@SnO_2/Ag, biological treatments including *Bacillus* (*B. cereus*, entre outros), Pseudomonas (Pseudomonas resinovorans, Pseudomonas fluorescents, P. psedudoalcaligenes), Alcaligenes, Klebsiella pneumonia, Rhodococcus sp., and Ralstonia sp., and fungi such as Trametes versicolor.[16,18,19]

2. EXPERIMENTAL SECTION

2.1. Materials and Physical Measurements. All materials were purchased from Aldrich and Merck chemical companies. Spectra of the Fourier Transform Infrared (FT-IR) were recorded as KBr tablets by PerkinElmer Spectrum (Version 10.02.00). ^{1}H NMR and ^{13}C NMR spectra were determined by an H 300MHz-3 Bruker AVANCE3-100MHz C instrument. Thermo Gravimetric Analysis (TGA) was recorded from room temperature to 800 °C using a TA-USA-Q600 instrument. Scanning electron microscopy (SEM) images were determined using an FE-SEM-Tescan-Czech Republic-Mira III instrument. The analysis of Energy Dispersive X-ray (EDX) was applied with an FE-SEM Tescan-France-Mira II ditector Samx instrument. Our recently reported educational synthetic organic methodology is useful for synthesis of desired compounds.[20]

2.2. Preparation of Biochar. In order to synthesize nanocatalyst based on biochar, olive mill pomace (OMP) was chosen as biomass according to the following procedure. At the first step, olive was washed and its kernel removed. The OMP at ambient air temperature was left to dry. After drying, the aggregates were softly crushed, and the particles were sieved to pass through a 1 cm sieve to ensure uniform and smooth size. Then biochar was produced by a slow pyrolysis process from air-dried OMP (1 h at 450 °C with a heating rate of 10 °C min^{-1}) using a furnace in the absence of air (oxygen). The obtained biochar was dried at 90 °C for 6 h.[21]

2.3. Synthesis of Cu-L-histidine@biochar. For functionalization of biochar by L-histidine, 1 g of biochar was dispersed in 100 mL of water for 30 min. Then 2 g of L-histidine was added to the reaction mixture. The reaction mixture was stirred under reflux conditions for 15 h. Then the resulting solid was filtered, washed with deionized water several times and dried at 50 °C. Finally, for metalation of L-histidine@biochar, 0.5 g of L-histidine@biochar was dispersed in 30 mL of absolute EtOH for 20 min and 0.25 g of $Cu(OAc)_2{\cdot}H_2O$ was added to the mixture under reflux conditions for 24 h. After filtration, the separated solid was washed with EtOH and water several times and dried at 50 °C overnight. Finally, the desired catalyst (Cu-L-histidine@biochar) was obtained (Scheme 1).

2.4. General Procedure for the Synthesis of Aniline Derivatives. Nitroarene (1 mmol), sodium tetrahydridoborate (5 mmol, 0.189 g) and 0.04 g of catalyst were added to a round-bottomed flask in water and stirred at 90 °C. For observation of the progress of the reaction, a TLC technique (*n*-hexane/ethyl acetate: 8/2) was used. When the reaction is completed, in order to remove the catalyst, it was separated by filter paper and washed with hot ethyl acetate, ethanol, and water. Then the oily product is separated with a decanter funnel. After evaporation, the aromatic amino products remain in the container. The model reaction is shown in Scheme 2.

Scheme 2. Model Reaction for the Nitroarenes Reduction

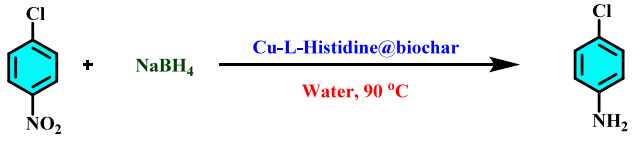

2.5. General Procedure for the Synthesis of Benzamide Compounds. In a round-bottomed flask, aromatic benzonitrile (1 mmol), potassium hydroxide (2 mmol, 0.112 g), and 0.04 g of catalyst were mixed at reflux of *n*-propanol. The reaction progress was checked by a TLC technique (*n*-hexane/ethyl acetate: 8/2). After completion of the reaction, the catalyst was separated by filtration and washed

https://doi.org/10.1021/acsomega.4c08465
ACS Omega 2024, 9, 47811−47821

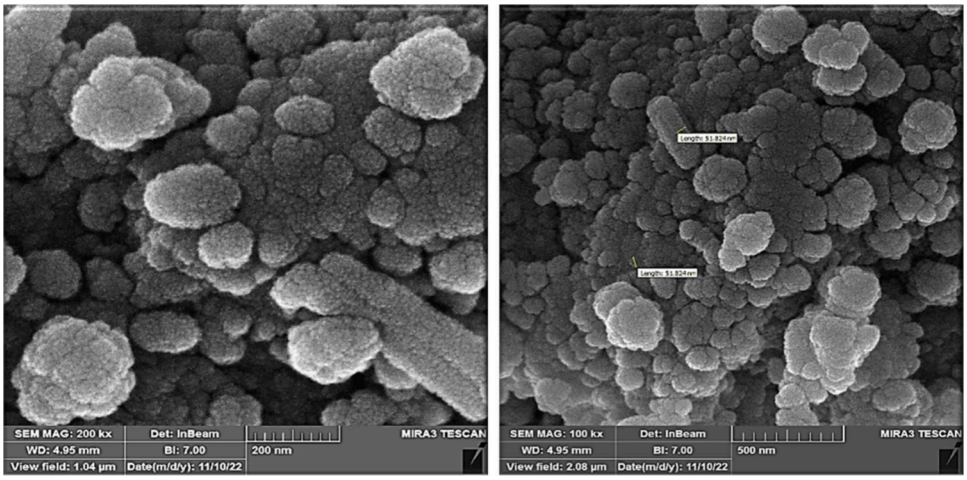

Figure 1. FE-SEM images of Cu-L-histidine@biochar.

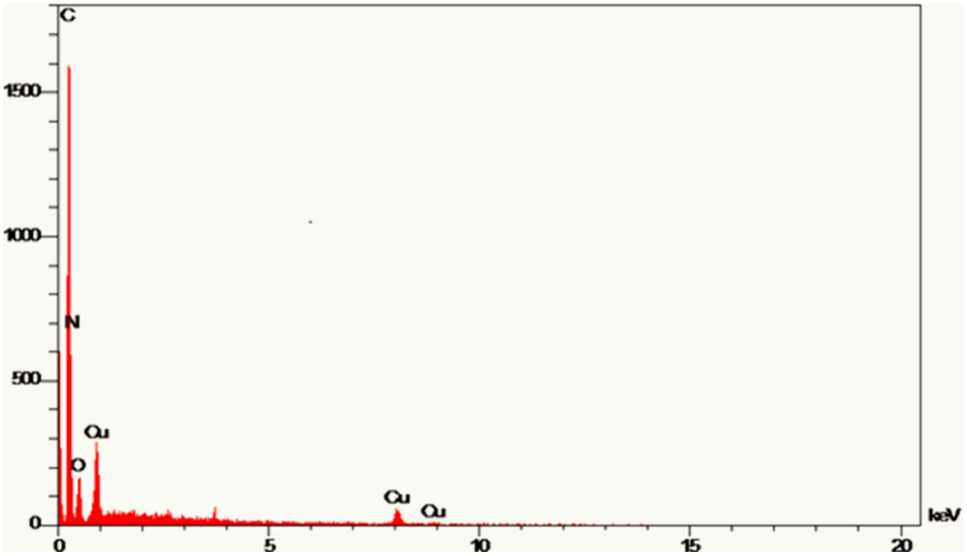

Figure 2. EDS spectrum of Cu-L-histidine@biochar.

with hot ethyl acetate. Ethanol and water were separated by a decanter funnel to achieve an oily benzamide product. The model reaction is shown in Scheme 4, derivatives of this reaction are presented in Table 3, and the optimal condition result is shown in Table 4.[22]

2.6. Selected Spectral Data. These compounds have been characterized by the ^{1}H NMR, ^{13}CNMR and FT-IR techniques:

4-Choloroaniline. FT- IR (KBr) cm^{-1}: 3368, 3179, 1659, 1407. ^{1}H NMR (300 MHz, *CDCl*$_3$) δ_{ppm} = 7.02 (d, *J* = 8.7 Hz, 2H), 6.53 (d, *J* = 8.7 Hz, 2H), 3.42 (s, 2H). ^{13}C NMR (100 MHz, *CDCl*$_3$) δ_{ppm} 144.9, 129.1, 123.2, 116.3.

(2-Aminophnyl) Methanol. FT- IR (KBr) cm^{-1}: 3392, 3204, 3192, 1606, 1495.[23] ^{1} H NMR (300 MHz, *D*$_2$*O*) δ_{ppm} 7.05 (t, *J* = 7.7 Hz, 1H), 6.96 (d, J = 7.4 Hz, 1H), 6.66−6.58 (m, 2H), 4.52 (s, 2H). ^{1}H NMR (300 MHz, *CDCl*$_3$) δ_{ppm} 7.05 (t, *J* = 7.7 Hz, 1H), 6.96 (d, *J* = 7.3 Hz, 1H), 6.67−6.59 (m, 2H), 4.54 (s, 2H), 4.43 (s, 1H), 3.44 (s, 2H).^{13}C NMR (100 MHz, *CDCl*$_3$) δ_{ppm} 145.5, 129.4, 129.3, 125.2, 118.6, 116.4, 64.2.

4-Chlorobenzamide. FT- IR (KBr) cm^{-1}: 3370, 3175, 2295, 1698, 1408. ^{1}H NMR (300 MHz, *DMSO*) δ_{ppm} 8.08 (s, 2H), 7.91 (d, *J* = 8.5 Hz, 2H), 7.56 (d, *J* = 8.5 Hz, 2H). ^{13}C NMR (100 MHz, *DMSO*) δ_{ppm} 167.3, 136.5, 133.5, 129.9, and 128.7.

4-Cyanobenzamide. FT- IR (KBr) cm^{-1}: 3380, 3213, 2238, 1713, 1667, 1409.^{1}H NMR (300 MHz, *DMSO*) δ_{ppm} = 8.30 (s, 2H), 8.04 (s, 2H), 7.98 (s, 2H). ^{13}CNMR (100 MHz, *DMSO*) δ_{ppm}: 169.7, 134.8, 133.2, 133.1, 132.7, 123.4.

2-Cyanobenzamide. FT- IR (KBr) cm^{-1}: 3381, 3204, 2919, 2236, 1667, 1407. ^{1}H NMR (300 MHz, *D*$_2$*O*) δ_{ppm} 7.96 (s, 1H), 7.78 (s, 2H), 7.69 (s, 1H). ^{1}H NMR (300 MHz, *DMSO*) δ_{ppm} = 9.65 (s, 2H), 8.06 (s, 1H), 7.84 (s, 2H), 7.71 (s, 1H). ^{13}CNMR (100 MHz, *DMSO*) δ_{ppm} 167.7, 166.9, 138.7, 137.0, 132.8, 128.8, 127.9, 114.1.

In order to define the result of the described reaction, we can refer to the positive effect of electrodonating groups in ortho and para regions on speed and yield of reaction. Also, the positive effect of the resonance is crystal clear.

3. RESULTS AND DISCUSSION

Development of synthetic organic methodologies, reagents, and catalysts is our main research interest. In this regard, we decided to synthesize a new catalyst for the reduction of

https://doi.org/10.1021/acsomega.4c08465
ACS Omega 2024, 9, 47811−47821

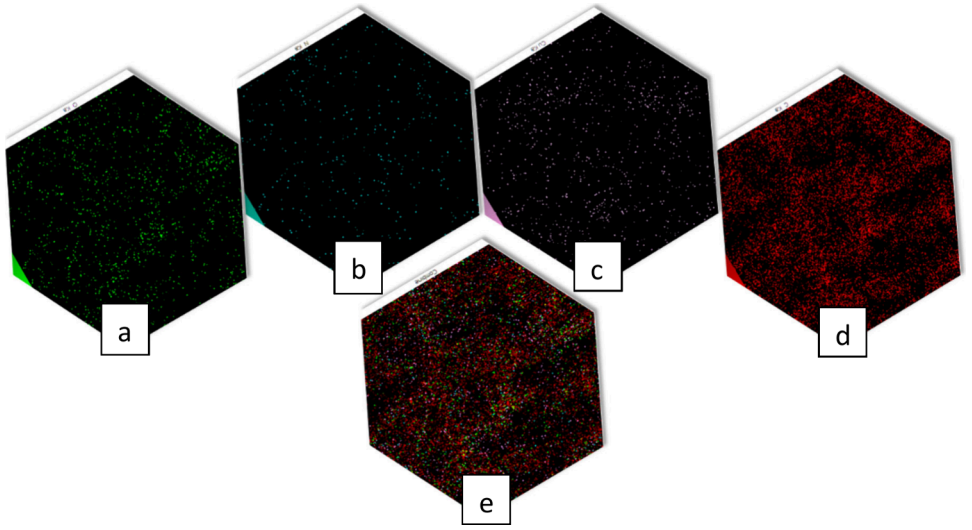

Figure 3. Elemental mapping of (a) oxygen, (b) nitrogen, (c) copper, (d) carbon, and (e) the combination of elements in Cu-L-histidine@biochar.

benzonitriles and benzonitriles. Herein, L-histidine is used as an amino acid for the modification of biochar, and then its complexation with Cu makes it an efficient catalyst for the conversion of nitroarene and benzonitriles to their corresponding amines and amides.

3.1. Catalyst Preparation. In order to synthesize the nanocatalyst based on biochar, olive mill pomace (OMP) was chosen as biomass. The prepared biochar was dispersed in deionized water, and then L-histidine was added to modify L-histidine@biochar nanoparticles. Finally, by adding $Cu(OAc)_2$. H_2O, the nanocatalyst was prepared as Cu-L-histidine@biochar.

3.2. Catalyst Characterization. In order to characterize the catalyst and after preparation, we probed the results by means of FT-IR, ICP, XRD, TGA, FE-SEM and EDS analysis.

The results of the FE-SEM technique are presented in Figure 1, which shows the morphology and the microstructure image from the surface of the catalyst. The images show the quasi-spherical shapes of catalyst particles, with about 50 nm in size. The particles of the presented catalyst had a good homogeneity in shape and size.[24]

EDS analysis determined the presence of Cu, O, N and C elements in biochar catalysts. It is worth mentioning that Cu was perfectly loaded on the biochar (Figure 2).

The element content of the catalyst, Cu-L-histidine@biochar, was made of oxygen, nitrogen, copper, and carbon, which shows a good homogeneous distribution of elements on the surface and in the structure of the desired catalyst (Figure 3).

The FT-IR spectra of the novel catalyst are shown step by step in Figure 4. In this figure, four spectra, A–D, are clearly visible. A is related to the olive biochar, which peaks at 3417 cm^{-1}, corresponding to hydrogen-bonded O–H stretching, and the symmetric C–O stretching appears at 1269 and 1596 cm^{-1} Also we have some aliphatic peaks at 2928 cm^{-1}. In the spectrum of pure L-histidine (Figure 4(B)), the characteristic NH_2 and carboxylic acid stretching frequencies are observed at 2500–3200 cm^{-1}, and asymmetric and symmetric stretching frequencies of carboxylate (COO^-) are observed at 1644 cm^{-1} υ_{as} (COO^-) and 1415 cm^{-1} υ_s (COO^-), respectively. The C spectrum confirms the grafting of L-histidine on the biochar, with peaks of the biochar present as well as the C–H aliphatic

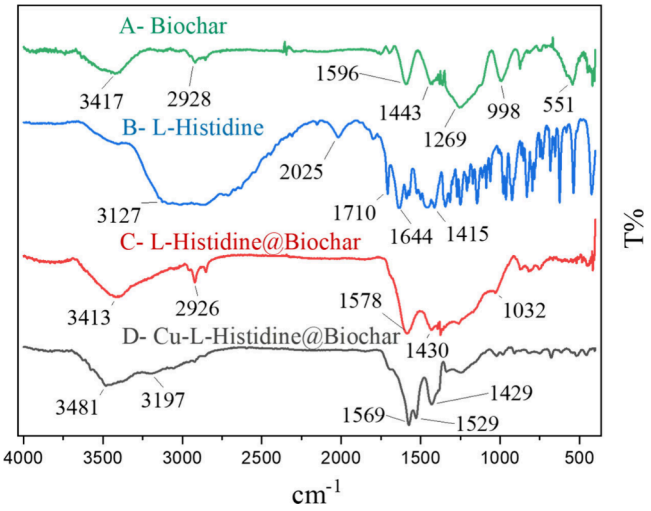

Figure 4. FT-IR spectra for the production of Cu-L-histidine@biochar.

peaks being preserved. Also, the asymmetric stretching vibration of the C–H groups of the imidazole ring and the aliphatic stretching vibration of C–H are indicated at 2926 cm^{-1}. Spectrum D shows the final structure of the catalyst, in which all mentioned peaks are preserved. (Figure 4).[25]

Thermogravimetric analysis (TGA), a method that measures the change in mass of a sample during a temperature rise, also indicates the thermal stability of the catalyst. As a result of TGA in this project, it was shown that at low temperatures below 150 °C, due to the removal of physically absorbed water and evaporation of solvents, the weight loss is slightly reduced (7% was observed). It can be seen that the weight loss of about 17% at the temperature of 200–550 °C helps the thermal decomposition of the immobilized L-histidine component in biochar, and the catalyst shows thermal stability up to a temperature of 250 °C (Figure 5).[26]

The powder X-ray diffraction pattern (XRD) indicated several peaks for modified biochar nanoparticles. The broad and strongest peak at 2θ = 20–30° is due to the crystal plane index C (0 0 2), which, in turn, is related to the parallel and azimuthal orientation of the aromatic and carbonized structure

https://doi.org/10.1021/acsomega.4c08465
ACS Omega 2024, 9, 47811–47821

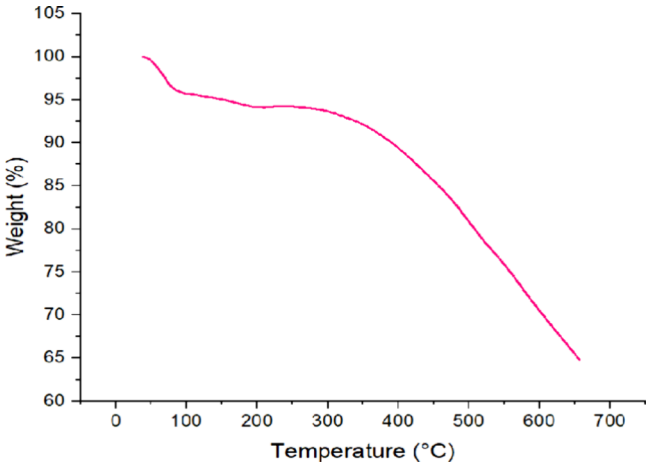

Figure 5. TGA diagram of Cu-L-histidine@biochar.

and is in agreement with the standard XRD pattern of biochar. Moreover, the presence of diffraction peaks located at 2θ = 40−50° reveals the presence of an amorphous structure of biochar (Figure 6).[27]

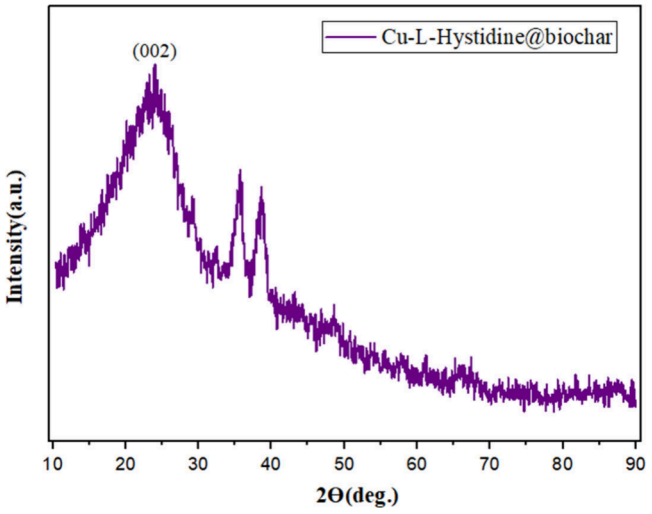

Figure 6. XRD diagram of Cu-L-histidine@biochar.

The amount of Cu by the ICP technique in Cu-L-histidine@biochar was investigated. The exact amount was 0.274 mmol/g.

To further investigate the chemical composition of Cu-L-histidine@biochar, XPS analysis was carried out. A measured XPS survey spectrum of the catalyst is illustrated in Figure 7(a), confirming the presence of Cu, N, O and C elements in the structure. In Figure 7(b), the N 1s spectrum could be curve-fitted into two components at 399 and 401 eV, interpreted as the nitrogen atom in the imidazole ring[28] and the interaction of Cu species with nitrogen.[29] Moreover, Figure 7(c) illustrates the Cu $2p_{3/2}$ and $2p_{1/2}$ spectra for the catalyst. The two peaks centered at 933.3 and the existence of a satellite peak were ascribed to the electron transition from the 3d to the 4s level through the relaxation process from the ligand to metal, confirming the characteristic of the Cu^{2+} state.[30] It is worth noting that the peak centered at 935 eV can be assigned to the $Cu(OAc)_2$, according to the analysis reported elsewhere.[31,32]

3.3. Catalytic Application. In order to investigate the catalyst application, we use it for the reduction of nitroarenes to aniline derivatives (Scheme 2) and also the conversion of nitriles to amides (Scheme 4). The optimal conditions for this conversion include temperature, time, solvent, and amount of catalyst probed, and the result is presented in Tables 1 and 2.

At first, the nitroarene reduction reaction is optimized. In this regard, *p*-chloronitroarene is used as a model reaction. The best conditions are achieved in the presence of 0.04 g of biochar catalyst and 5 mmol of $NaBH_4$ at 90 °C in water for 1 mmol of reactant. Different solvents such as water, ethanol, *n*-hexane, *N, N*-dimethylformamide, and ethanol/water in a ratio of 50% were investigated. The results showed that in *n*-hexane, DMF and solvent free conditions, there was no noticeable reaction. The temperature has a direct impact on the reaction, and a decrease up to room temperature gives 27% of the target product (Table 1, Entries 1−3). Under catalyst free conditions and using just a reducing agent, the reaction efficiency was very low (Table 1, Entry 14). The obtained results supported that the use of a catalyst is necessary for the reduction reaction, due to the absorption of hydride by the copper on L-histidine biochar (Scheme 3). Also, the amount of product was increased by increasing the amount of the presented catalyst (Table 1, Entries 3−5). An increase of catalyst to 0.05 g had a negative effect on the yield of product (Table 1, Entry 6), and a decrease to 0.03 g reduced it up to 52%. In another test, with 3 mmol of $NaBH_4$, the yield of the product reduced to 76% (Table 1, Entry 12).

It has been shown in Table 2 that all nitroarene reductions were successfully performed in high yields and short times. For nitrobenzaldehydes (Table 2, Entries 5 and 6) reduction happens on both sides of nitro and aldehyde. The interesting point of this catalytic reduction system is its chemoselectivity in the case of meta- and para-nitrobenzonitrile. As shown in Table2, entries 3 and 4, only the nitro group reduced, and CN remained intact (Scheme 5).

Herein, a possible mechanism for the reduction of nitrobenzene to aniline in the presence of Cu-L-histidine@biochar is proposed. First, BH_4^- ions were adsorbed at the catalyst surface (Scheme 3). Then Cu(II) tags accelerated the reduction reaction via accepting electrons from BH_4^-, so that the Cu(II) in situ is converted to Cu^0. This process of in situ Cu^0 formation would catalyze the reduction of nitrobenzene through the adsorption of nitrobenzene and hydride transfer. Finally, after electron transfer and desorption of aniline, Cu^0 was reoxidized to Cu(II). This process helped accelerate the catalytic reduction reaction.[37]

In another study, the conversion of nitriles to the corresponding amides was also examined (Scheme 4). For optimization of the reaction conditions, *p*-chlorobenzonitrile was chosen as a model reaction. Various solvents such as water, ethanol, *n*-propanol, 2-propanol and solvent free conditions were probed. Increasing the temperature improved the yield of the target reaction. As shown in Table 3 at 25 °C the product minimal. The use of catalyst more than 0.04 g has a hindering role in the reaction, and a decrease in the yield of the final product using 0.04 g of catalyst in *n*-propanol under reflux conditions and 2 mmol of KOH was observed.

Reduction reactions by different ranges of electron withdrawing and electron donating groups had a good yield, although for aliphatic compounds in conversion of cyanides no reaction occurred (Table 4). The mechanism of reaction is shown in Scheme 6.

https://doi.org/10.1021/acsomega.4c08465
ACS Omega 2024, 9, 47811−47821

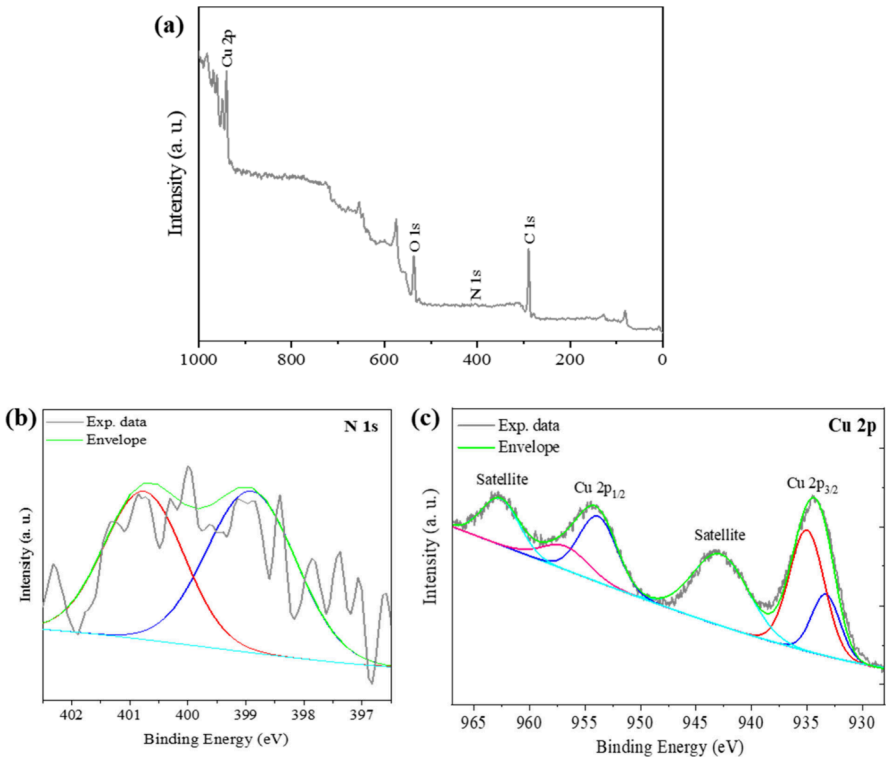

Figure 7. (a) XPS survey spectrum and deconvoluted core-level photoelectron spectra of (b) N 1s and (c) Cu 2p for Cu-L-histidine@biochar.

Table 1. Optimization of Reaction for the Nitroarene Reduction

Entry	*Solvent*	*Catalyst (g)*	*$NaBH_4$ (mmol)*	*Temp (°C)*	*Yield (%)*	*Time (min)*
1	Water	0.02	5	r.t	27	60
2	Water	0.04	5	50	75	90
3	**Water**	**0.04**	**5**	**90**	**94**	**40**
4	Water	0.02	5	90	44	180
5	Water	0.03	5	90	52	180
6	Water	0.05	5	90	64	100
7	Solvent free	0.04	5	90	Trace	120
8	Ethanol	0.04	5	90	63	120
9	*n*-Hexane	0.04	5	90	N.R	120
10	DMF	0.04	5	90	Trace	120
11	Water/ Ethanol	0.04	5	90	90	60
12	Water	0.04	3	90	76	106
13	Methanol	0.04	5	90	75	120
14	Water	-	5	90	41	180

According to our introducing homoselective concepts and also chemoselectivity,[46−52] the chemoselectivity, used for meta- and para-nitrobenzylnitriles (Table 2, Entries 3 and 4), and homoselectivity, used for phthalonitrile and terephthalonitrile (Table 4, Entries 4 and 5), were described. To examine the chemoselectivity, under the optimized reaction conditions, meta- and para-nitrobenzylnitriles were selected for reduction to aniline. The results showed that only the nitro group undergoes the reaction in this condition (Scheme 5). The homoselective reaction is used when two of the same functional groups are present within a molecule, and interestingly, only one is converted to a new group. Herein, the homoselectivity of the presented method was checked under the optimized reaction conditions in the reaction of

Table 2. Synthesis of Various Aniline Derivatives[a]

Entry	Nitroarenes	Product	TOF	Time(min)	Yield	M.P
1	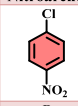	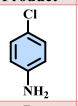	128	40	94%	70-73[33]
2	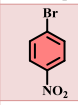	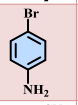	109	45	90%	65-68[33]
3	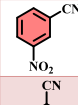	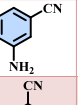	90	53	87%	51-54[33]
4	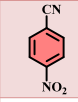	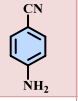	114	43	90%	80-84[33]
5	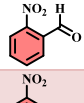	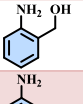	160	37	93%	78-81[34]
6	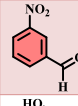	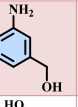	151	32	88%	86-89[33]
7		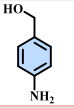	148	32	86%	62-63[35]
8	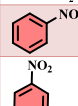	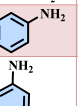	135	35	86%	Oil[33]
9	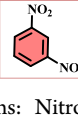	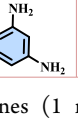	102	35	65%	68-73[36]

[a]Conditions: Nitroarenes (1 mmol), $NaBH_4$ (5 mmol, 0.189 g), catalyst (0.04 g), 90 °C, H_2O (10 mL).

phthalonitrile and terephthalonitrile, in which only one of the cyano groups was reduced, (Scheme 5). This fact was proven

https://doi.org/10.1021/acsomega.4c08465
ACS Omega 2024, 9, 47811−47821

Scheme 3. Suggested Mechanism for Nitroarene Reduction in the Presence of Catalyst

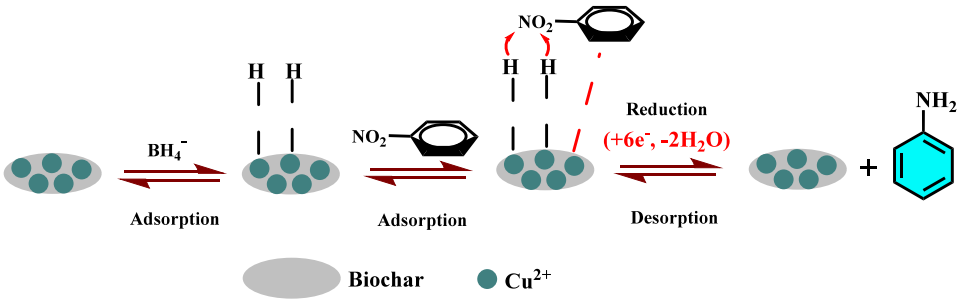

Scheme 4. Model Reaction for Aromatic Benzonitrile Reduction

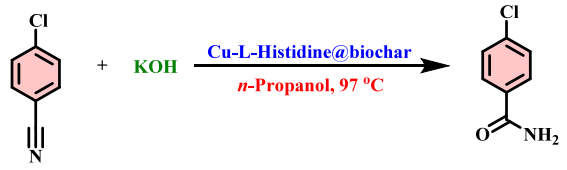

Table 3. Optimization of Reaction for Conversion of Benzonitriles

Entry	*Solvent*	*Catalyst (g)*	*KOH (mmol)*	*Temp (°C)*	*Yield (%)*	*Time (min)*
1	Water	0.04	2	70	30	104
2	Water	0.04	2	100	25	26
3	Ethanol	0.04	2	80	40	175
4	2-Propanol	0.04	2	97	Trace	185
5	**n-Propanol**	**0.04**	**2**	**97**	**98**	**120**
6	n-Propanol	0.04	1	97	50	60
7	n-Propanol	0.05	2	97	73	180
8	n-Propanol	0.03	2	97	41	85
9	n-Propanol	0.03	2	80	37	135
10	n-Propanol	0.04	2	80	50	200
11	n-Propanol	0.04	2	25	Trace	120
12	-	0.04	2	100	46	155
13	n-Propanol	0.02	2	97	70	120

by the existence of the peak of about 2200 in the IR spectrum of both products as well as the melting point; ^{1}H NMR and ^{13}CNMR support this fact. It should be noted that by doubling the amount of catalyst and KOH, only one of the groups was reduced again. In the case of aliphatic nitriles such as benzylnitrile, no product was found (Table 4, Entry 11).

A proposed mechanism for the hydration of benzonitriles to benzamides is shown in Scheme 6. Initially, coordination of benzonitrile to the Cu-catalyst increases the electrophilicity of the nitrile carbon (intermediate I), which upon addition of OH^- ion from KOH in alcoholic solution leads to an intermediate (II). Finally, the abstraction of a proton produces the corresponding amide as a desired product.[53]

Investigation of Efficiency of Cu-L-histidine@biochar. The turnover frequency (TOF) value is a significant factor to evaluate the performance of the catalyst, which indicates how many catalytic reaction cycles proceed per site and unit of time. Herein TOF was calculated for all products and is entered in Tables 2 and 4. Based on the result achieved from ICP and TOF obtained from yield, the amounts of catalyst (mol % of Cu) and time, the obtained values are acceptable and indicate the good efficiency of the presented catalyst.[54]

Table 4. Derivatives for the Synthesis of Benzamide Compounds[a,b]

Entry	Benzonitriles	Product	TOF	Time(min)	Yield	M.P
1		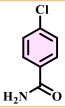	45	120	98%	173-175[38]
2			82	60	90%	124-129[39]
3		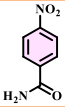	12	5.30 h	68%[b]	200-205[40]
4		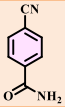	195	25	90%	178-180[41]
5			262	20	95%	220-224[42]
6			27	120	60%	142-145[38]
7			28	155	80%	143-145[43]
8		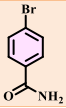	31	155	88%	192-194[38]
9		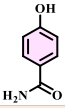	24	180	80%[b]	162-165[44]
10			8	180	25%[b]	142-147[45]
11		-	-	160	-	-

[a]Conditions: Benzonitriles derivatives (1 mmol), KOH (2 mmol, 0.112 g), catalyst (0.04 g), 97 °C, *n*-propanol (10 mL). [b]Reaction did not complete and was purified by plate chromatography.

Recyclability of the Catalyst. The reusability of the catalyst was also examined by reduction of *p*-choloronitrobenzene and hydration of *p*-chlorobenzonitrile as model reactions. After the reaction completion, the catalyst was easily recovered from the reaction mixture using simple filtration and then thorough washing with EtOH and water and drying at 50 °C for use in the next run. The catalyst was separated by filter paper and perfectly washed in order to be reused in the next reaction. As

https://doi.org/10.1021/acsomega.4c08465
ACS Omega 2024, 9, 47811−47821

Scheme 5. Chemo- and Homoselective Studies

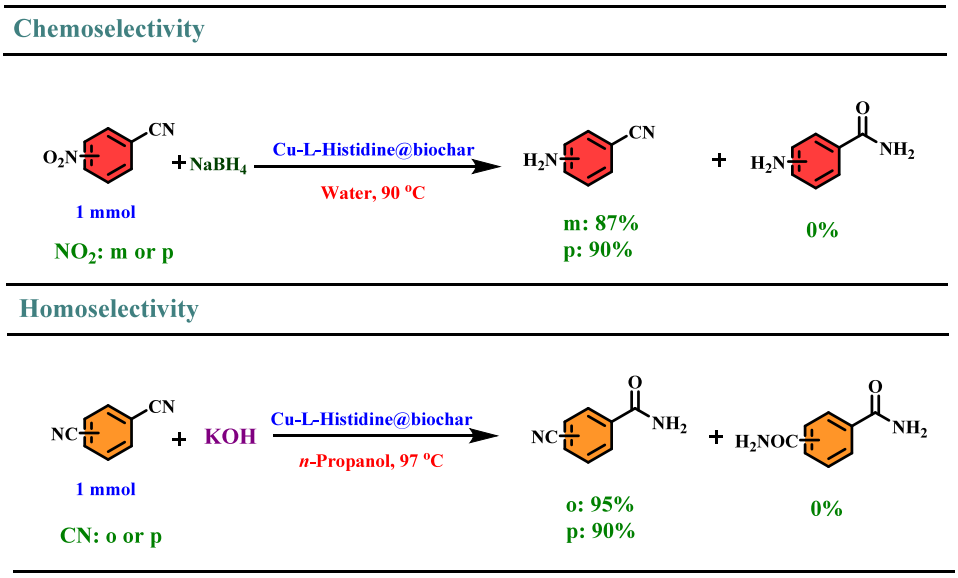

Scheme 6. Suggested Mechanism for Synthesis of Benzamide in the Presence of Catalyst

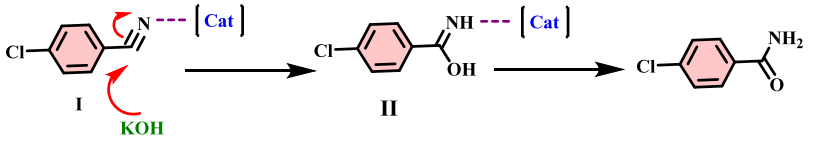

shown in Scheme 5 the recycled catalyst was used for up 4 runs without remarkable loss of its catalytic activity (Figure 8).

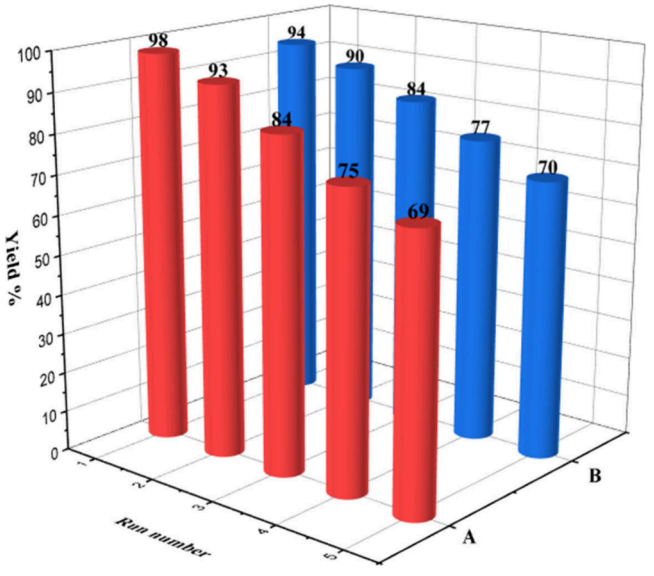

Figure 8. Catalyst recovery for *p*-chlorobenzonitrile (A) and *p*-choloronitrobenzene (B).

In order to explore the stability of Cu-L-histidine@biochar after recovery, the reused catalyst was characterized by the FT-IR spectrum. For the fresh catalyst and recovered catalyst, the peaks are located in the same areas. For example, the vibration of N−H was observed at 3481 cm^{-1}. Also, it can be seen that the structure of the catalyst was preserved after recovery (Figure 9).

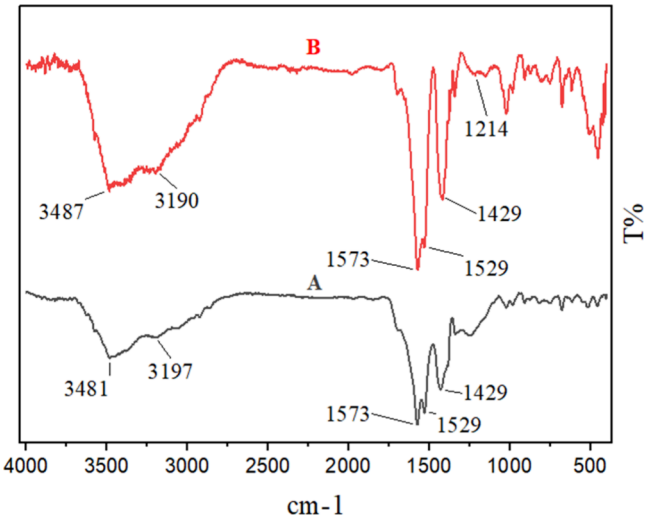

Figure 9. FT-IR spectra of Cu-L-histidine@biochar (A) and recovered Cu-L-histidine@biochar (B).

Compared with the fresh catalyst, the structure of the recovered catalyst was not destroyed, but a decrease in XRD peak intensity is an indication of a low degree of crystallinity and also a decrease in catalytic activity may be due to a slight loss of the catalyst active moiety and leaching after several uses (Figure 10).

4. HOT FILTRATION TEST

The heterogeneity of the catalyst was established by a hot filtration test. The reduction reaction of *p*-nitro benzyl alcohol as a substrate was investigated under optimized reaction conditions to determine the leaching of copper in the reaction

https://doi.org/10.1021/acsomega.4c08465
ACS Omega 2024, 9, 47811−47821

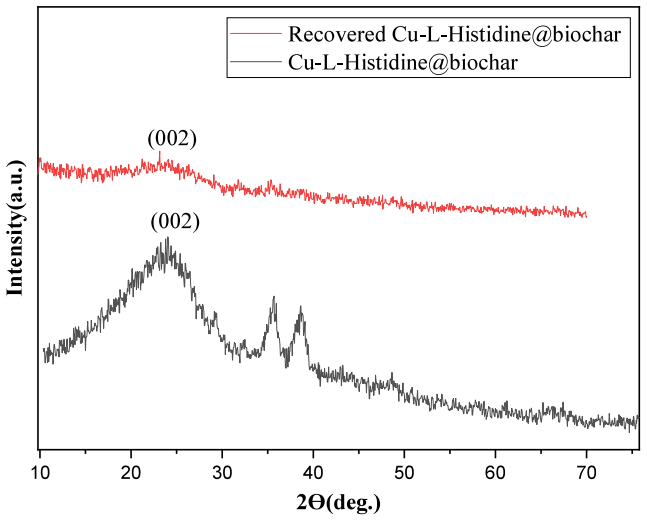

Figure 10. XRD diagram of Cu-L-histidine@biochar (bottom) and recovered Cu-L-histidine@biochar (top).

media. The catalyst was filtered off from the reaction mixture under hot conditions (at 90 °C) after 15 min, and the reaction was allowed to continue with the filtrate for another 15 min. The yield of the product in this experiment as determined by ^{1}HNMR was 52%. Then the parallel reaction was repeated, but in half the time of the reaction (15 min) the product was obtained by ^{1}HNMR in 33%. This result revealed no significant leaching of Cu during the reaction. The 1HNMR results are available in Supporting Information.

5. COMPARISON OF THE CATALYST

In order to indicate the catalytic activity of Cu-L-histidine@biochar, we compared the results for the synthesis of benzamides and anilines in the presence of the described catalyst with previously reported methods in the literature (Tables 5 and 6). These results show that Cu-L-histidine@biochar affords a short reaction time and higher yield than other catalysts.

Table 5. Comparison of the Performance of Different Catalysts in the Synthesis of Benzamide Compounds

Entry	Benzonitriles	Product	Catalyst	Temperature (°C)	Time	Yield
1		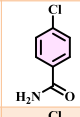	Cu-L-histidine@biochar	97	2h	98%
2		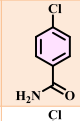	Rh	25	17h	90% [55]
3		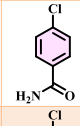	Fe_3O_4@SiO_2–NHC–Cu (II)	110	6h	96% [56]
4		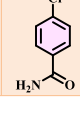	Ru $(OH)_x/Al_2O_3$	140	10-24h	77-98% [57]

Table 6. Comparison of the Performance of Different Catalysts in the Synthesis of Aniline Derivatives

Entry	Nitroarenes	Product	Catalyst	Temperature (°C)	Time	Yield
1			Cu-L-histidine@biochar	90	0.6h	94%
2			DMSO-Tagged Molecular Cobalt Corrole Catalyst	120	15h	99% [58]
3			Ni_3Sn_2/TiO_2	150	12h	100% [59]
4			1,1,3,3-tetramethyldisiloxane	60	48h	99% [60]

6. CONCLUSIONS

In summary, we have designed Cu-L-histidine@biochar from inexpensive renewable resources as an efficient catalyst for the coselective chemical reduction of nitroarenes and the hydration of benzonitriles to the corresponding amines and amides. The advantages of the catalyst are easy preparation and operation without tedious conditions, environmental friendliness, low toxicity, and operability. More importantly, the catalyst can be easily separated using simple filtration and recycled several times without a loss of functionality. In addition, the obtained products were synthesized in relatively short time, high efficiency, relatively green conditions, and low temperature.

■ ASSOCIATED CONTENT

Data Availability Statement

The data sets used and/or analyzed during the present study are available from the corresponding author upon reasonable request. All data generated or analyzed during this study are included in this published article and its Supporting Information files.

Supporting Information

The Supporting Information is available free of charge at https://pubs.acs.org/doi/10.1021/acsomega.4c08465.

Spectra for IR, ^{1}HNMR and ^{13}CNMR of some benzamide and aniline derivatives, ^{1}HNMR of Hot filtration test results. (PDF)

■ AUTHOR INFORMATION

Corresponding Authors

Maryam Hajjami − *Department of Organic Chemistry, Faculty of Chemistry and Petroleum Sciences, Bu-Ali Sina University, Hamedan 6517838683, Iran;* orcid.org/0000-0002-5225-4809; Phone: +988138282807; Email: m.hajjami@basu.ac.ir, mhajjami@yahoo.com; Fax: +988138380709

Mohammad Ali Zolfigol − *Department of Organic Chemistry, Faculty of Chemistry and Petroleum Sciences, Bu-Ali Sina University, Hamedan 6517838683, Iran;* orcid.org/0000-0002-4970-8646; Phone: +988138282807; Email: zolfi@basu.ac.ir, mzolfigol@yahoo.com; Fax: +988138380709

https://doi.org/10.1021/acsomega.4c08465
ACS Omega 2024, 9, 47811−47821

Authors

Mahrokh Farrokh − *Department of Organic Chemistry, Faculty of Chemistry and Petroleum Sciences, Bu-Ali Sina University, Hamedan 6517838683, Iran*

Sepideh Jalali-Mola − *Department of Organic Chemistry, Faculty of Chemistry and Petroleum Sciences, Bu-Ali Sina University, Hamedan 6517838683, Iran*

Complete contact information is available at: https://pubs.acs.org/10.1021/acsomega.4c08465

Notes

The authors declare no competing financial interest.

■ ACKNOWLEDGMENTS

The authors thank Bu-Ali Sina University for the financial support for this research.

■ REFERENCES

(1) Yang, Y.; Chiang, K. Porous carbon-supported catalysts for energy and environmental applications: A short review. *Catal. Today.* **2011**, *178* (1), 197−205.

(2) Moradi, P.; Hajjami, M.; Tahmasbi, B. Fabricated copper catalyst on biochar nanoparticles for the synthesis of tetrazoles as antimicrobial agents. *Polyhedron.* **2020**, *175*, No. 114169.

(3) Moradi, P.; Hajjami, M. Stabilization of ruthenium on biochar-nickel magnetic nanoparticles as a heterogeneous, practical, selective, and reusable nanocatalyst for Suzuki C-C coupling reaction in water. *RSC Adv.* **2022**, *12*, 13523−13534.

(4) Aazza, M.; Ahlafi, H.; Moussout, H.; Mounir, C.; Fadel, A.; Addad, A. Catalytic reduction of nitro-phenolic compounds over Ag, Ni and Co nanoparticles catalysts supported on γ-Al2O3. *J. Environ. Chem. Eng.* **2020**, *8* (2), No. 103707.

(5) Albanio, I. I.; Muraro, P. C. L.; da Silva, W. L. Rhodamine B dye adsorption onto biochar from olive biomass waste. *Water, Air, & Soil Pollution.* **2021**, *232* (5), 214.

(6) Goswami, L.; Kushwaha, A.; Singh, A.; Saha, P.; Choi, Y.; Maharana, M.; Kim, B. S. Nano-biochar as a sustainable catalyst for anaerobic digestion: a synergetic closed-loop approach. *Catal.* **2022**, *12* (2), 186.

(7) Chen, W.; Meng, J.; Han, X.; Lan, Y.; Zhang, W. Past, present, and future of biochar. *Biochar.* **2019**, *1* (1), 75−87.

(8) Li, Z.; Xing, B.; Ding, Y.; Li, Y.; Wang, S. A high-performance biochar produced from bamboo pyrolysis with in-situ nitrogen doping and activation for adsorption of phenol and methylene blue. *Chin. J. Chem. Eng.* **2020**, *28* (11), 2872−2880.

(9) Wang, J.; Wang, S. Preparation, modification and environmental application of biochar: a review. *J. Clean. Prod.* **2019**, *227*, 1002−1022.

(10) Tonouchi, N.; Ito, H. Present global situation of amino acids in industry. *Amino Acid Fermentation.* **2016**, *159*, 3−14.

(11) Yang, Q.; Sherbahn, M.; Runge, T. Basic amino acids as green catalysts for isomerization of glucose to fructose in water. *ACS Sustain. Chem. Eng.* **2016**, *4* (6), 3526−3534.

(12) Sang Sefidi, V.; Luis, P. Advanced amino acid-based technologies for CO_2 capture: a review. *Ind. Eng. Chem. Res.* **2019**, *58* (44), 20181−20194.

(13) Cortes-Clerget, M.; Lee, N. R.; Lipshutz, B. H. Synthetic chemistry in water: applications to peptide synthesis and nitro-group reductions. *Nat. Protoc.* **2019**, *14* (4), 1108−1129.

(14) Sun, S.; Quan, Z.; Wang, X. Selective reduction of nitro-compounds to primary amines by nickel-catalyzed hydrosilylative reduction. *RSC adv.* **2015**, *5* (103), 84574−84577.

(15) Moradi, P.; Hajjami, M. Magnetization of biochar nanoparticles as a novel support for fabrication of organo nickel as a selective, reusable and magnetic nanocatalyst in organic reactions. *New J. Chem.* **2021**, *45* (6), 2981−2994.

(16) Pan, Y.; Zhang, Y.; Huang, Y.; Jia, Y.; Chen, L. Enhanced photocatalytic oxidation degradability for real cyanide wastewater by designing photocatalyst GO/TiO2/ZSM-5: Performance and mechanism research. *J. Chem. Eng.* **2022**, *428*, No. 131257.

(17) Guo, Y.; Wang, Y.; Zhao, S.; Liu, Z.; Chang, H.; Zhao, X. Photocatalytic oxidation of free cyanide over graphitic carbon nitride nanosheets under visible light. *J. Chem. Eng.* **2019**, *369*, 553−562.

(18) Alvillo-Rivera, A.; Garrido-Hoyos, S.; Buitrón, G.; Thangarasu-Sarasvathi, P.; Rosano-Ortega, G. Biological treatment for the degradation of cyanide: A review. *JMR&T.* **2021**, *12*, 1418−1433.

(19) Liu, D.; Jin, C.; Zhang, Y.; He, Y.; Wang, F. Integrated piezo-photocatalysis of electrospun Bi4Ti3O12 nanostructures by bi-harvesting visible light and ultrasonic energies. *Ceram. Int.* **2021**, *47* (6), 7692−7699.

(20) Zolfigol, M. A.; Azizian, S.; Torabi, M.; Yarie, M.; Notash, B. The Importance of Nonstoichiometric Ratio of Reactants in Organic Synthesis. *J. Chem. Educ.* **2024**, *101*, 877.

(21) Hmid, A.; Mondelli, D.; Fiore, S.; Fanizzi, F. P.; Al Chami, Z.; Dumontet, S. Production and characterization of biochar from three-phase olive mill waste through slow pyrolysis. *Biomass and bioenergy.* **2014**, *71*, 330−339.

(22) Berenguer, R.; Quijada, C.; La Rosa-Toro, A.; Morallón, E. Electro-oxidation of cyanide on active and non-active anodes: Designing the electrocatalytic response of cobalt spinels. *Sep. Purif. Technol.* **2019**, *208*, 42−50.

(23) Sundaraganesan, N.; Saleem, H.; Mohan, S.; Ramalingam, M. FT-Raman and FTIR spectra, assignments and ab initio calculations of 2-aminobenzyl alcohol. *Spectrochim. Acta. A: Mol. Biomol Spectrosc.* **2005**, *61* (3), 377−385.

(24) Norouzi, M.; Moradi, P. A new copper complex on functionalized magnetic biochar nano-sized materials as sustainable heterogeneous catalysts for C−O bond formation in the natural deep eutectic solvent. *Biomass Conversion and Biorefinery.* **2023**, 1−13.

(25) Azadi, G.; Ghorbani-Choghamarani, A.; Shiri, L. Copper (II) immobilized on Fe 3 O 4@ SiO 2@ l-Histidine: A reusable nanocatalyst and its application in the synthesis of 5-substituted 1 H-tetrazoles. *Transit. Met. Chem.* **2017**, *42*, 131−136.

(26) Rashidi, S.; Gholamian, F.; Hajjami, M. Immobilization of Ni(II)-4-phenylthiosemicarbazide into functionalized MCM-41 as nano catalyst in synthesis of tetrahydrobenzo[b]pyran and 1,4-dihydropyrano[2,3-c]pyrazole. *J. Nanoparticle res.* **2023**, *25*, 102−120.

(27) Yeboah, M. L.; Li, X.; Zhou, S. Facile fabrication of biochar from palm kernel shell waste and its novel application to magnesium-based materials for hydrogen storage. *Mater.* **2020**, *13* (3), 625.

(28) Rezaei, A.; Hadian-Dehkordi, L.; Samadian, H.; Jaymand, M.; Targhan, H.; Ramazani, A.; Adibi, H.; Deng, X.; Zheng, L.; Zheng, H. Pseudohomogeneous metallic catalyst based on tungstate-decorated amphiphilic carbon quantum dots for selective oxidative scission of alkenes to aldehyde. *Sci. Rep.* **2021**, *11*, 4411−4423.

(29) Bulushev, D. A.; Chuvilin, A. L.; Sobolev, V. I.; Stolyarova, S. G.; Shubin, Y. V.; Asanov, I. P.; Ishchenko, A. V.; Magnani, G.; Ricco, M.; Okotrub, A. V.; Bulusheva, L. G. Copper on carbon materials: stabilization by nitrogen doping. *J. mater. Chem. A* **2017**, *5*, 10574−10583.

(30) Mureseanu, M.; Puscasu, M. C.; Somacescu, S.; Carja, G. CuII(Sal-Ala)/CuAlLDH Hybrid as Novel Efficient Catalyst for Artificial Superoxide Dismutase (SOD) and Cyclohexene Oxidation by H_2O_2. *Catal. Lett.* **2015**, *145* (8), 1529−1540.

(31) Jiang, M.; Tuo, Y.; Cai, M. Immobilization of copper(II) on mesoporous MCM-41: a highly efficient and recyclable catalyst for tandem oxidative annulation of amidines and methylarenes. *J. Porous Mater.* **2020**, *27* (4), 1039−1049.

(32) Moulder, J. F.; Stickle, W. F.; Sobol, P. E.; Bomben, K. D.; Chastain, J. In *Handbook of X-Ray Photoelectron Spectroscopy: A Reference Book of Standard Spectra for Identification and Interpretation of XPS Data*; Chastain, J., Ed.; Perkin-Elmer Corporation, Waltham, 1992.

https://doi.org/10.1021/acsomega.4c08465
ACS Omega 2024, 9, 47811−47821

(33) Moradi, Z.; Ghorbani-Choghamarani, A. Fe3O4@ SiO2@ KIT-6@2-ATP@CuI as a catalyst for hydration of benzonitriles and reduction of nitroarenes. *Sci. Rep.* **2023**, *13* (1), 7645.
(34) Mirbagheri, R.; Elhamifar, D. Magnetic ethyl-based organosilica supported Schiff-base/indium: A very efficient and highly durable nanocatalyst. *J. Alloys Compd.* **2019**, *790*, 783−791.
(35) Zeynizadeh, B.; Sepehraddin, F. Synthesis and characterization of magnetically nanoparticles of Fe 3 O 4@ APTMS@ ZrCp 2 as a novel and reusable catalyst for convenient reduction of nitro compounds with glycerol. *JICS.* **2017**, *14*, 2649−2657.
(36) Kandathil, V.; Koley, T. S.; Manjunatha, K.; Dateer, R. B.; Keri, R. S.; Sasidhar, B. S.; Patil, S. A. A new magnetically recyclable heterogeneous palladium (II) as a green catalyst for Suzuki-Miyaura cross-coupling and reduction of nitroarenes in aqueous medium at room temperature. *Inorg. Chim. Acta* **2018**, *478*, 195−210.
(37) Tang, J.; Zhang, S.; Chen, X.; Zhang, L.; Du, L.; Zhao, Q. Highly Efficient Catalytic Reduction of Nitrobenzene Using Cu@ C Based on a Novel Cu−MOF Precursor. *Catal.* **2023**, *13* (6), 956.
(38) Kalimani, F. M.; Khorshidi, A. Ag-embedded manganese oxide octahedral molecular sieve (Ag-OMS-2) nano-rods as efficient heterogeneous catalysts for hydration of nitriles to amides in aqueous solution. *RSC adv.* **2023**, *13* (10), 6909−6918.
(39) Xia, C.; Chen, X.; Dai, J.; Gao, F.; Wang, N.; Wang, J.; Hong, B. Cyanation and Hydrolysis Cascade of Aryl Bromides with Cuprous Cyanide to Access Primary Amides. *Synlett.* **2023**, *34* (17), 1991−1996.
(40) Nirmala, M.; Adinarayana, M.; Ramesh, K.; Maruthupandi, M.; Vaddamanu, M.; Raju, G.; Prabusankar, G. Water-soluble superbulky (η 6-p-cymene) ruthenium (ii) amine: an active catalyst in the oxidative homocoupling of arylboronic acids and the hydration of organonitriles. *New J. Chem.* **2018**, *42* (18), 15221−15230.
(41) Popova, M.; Trendafilova, I.; Tsacheva, I.; Mitova, V.; Kyulavska, M.; Koseva, N.; Szegedi, A. Amino-modified KIT-6 mesoporous silica/polymer composites for quercetin delivery: Experimental and theoretical approaches. *Microporous Mesoporous Mater.* **2018**, *270*, 40−47.
(42) Kazemi Miraki, M.; Arefi, M.; Salamatmanesh, A.; Yazdani, E.; Heydari, A. Magnetic nanoparticle-supported Cu−NHC complex as an efficient and recoverable catalyst for nitrile hydration. *Catal. Lett.* **2018**, *148*, 3378−3388.
(43) Das, S. K.; Bhattacharjee, P.; Sarmah, M.; Kakati, M.; Bora, U. A sustainable approach for hydration of nitriles to amides utilising WEB as reaction medium. *CRGSC* **2021**, *4*, No. 100071.
(44) Ma, X.; Lu, M. Copper (II) acetate-catalysed conversion of aldoximes to amides under mild conditions. *J. Chem. Res.* **2016**, *40* (10), 594−596.
(45) Joarder, D. D.; Gayen, S.; Sarkar, R.; Bhattacharya, R.; Roy, S.; Maiti, D. K. (Ar-tpy) RuII (ACN) 3: A Water-Soluble Catalyst for Aldehyde Amidation, Olefin Oxo-Scissoring, and Alkyne Oxygenation. *J. Org. Chem.* **2019**, *84* (13), 8468−8480.
(46) Zolfigol, M. A.; Amani, K.; Ghorbani-Choghamarani, A.; Hajjami, M.; Ayazi-Nasrabadi, R.; Jafari, S. Chemo and homoselective catalytic oxidation of sulfides to sulfoxides with supported nitric acid on silica gel and poly vinyl pyrrolidone (PVP) catalyzed by KBr and/or NaBr. *Catal. Commun.* **2008**, *9* (8), 1739−1744.
(47) Amani, K.; Zolfigol, M. A.; Ghorbani-Choghamarani, A.; Hajjami, M. Ferric nitrate in the presence of catalytic amounts of KBr or NaBr: an efficient and homoselective catalytic media for the selective oxidation of sulfides to sulfoxides. *Monatsh. Chem.* **2009**, *140*, 65−68.
(48) Safaiee, M.; Moeinimehr, M.; Zolfigol, M. A. Pyridiniumporphyrazinato oxo-vanadium tribromomethanide as a new source of Br+ catalyst for the chemo and homoselective oxidation of sulfides and benzylic alcohols. *Polyhedron.* **2019**, *170*, 138−150.
(49) Chehardoli, G.; Zolfigol, M. A. Melamine Hydrogen Peroxide (MHP): Novel and Efficient Reagent for the Chemo-and Homoselective and Transition Metal−Free Oxidation of Thiols and Sulfides. *Phosphorus, Sulfur, and Silicon.* **2009**, *185* (1), 193−203.
(50) Sepehrmansourie, H.; Zarei, M.; Zolfigol, M. A.; Kalhor, S.; Shi, H. Catalytic chemo and homoselective ipso-nitration under mild condition. *Mol. Catal.* **2022**, *531*, No. 112634.
(51) Dehbanipour, Z.; Moghadam, M.; Tangestaninejad, S.; Mirkhani, V.; Mohammadpoor-Baltork, I. Chloromethylated polystyrene supported copper (II) bis−thiazole complex: Preparation, characterization and its application as a heterogeneous catalyst for chemoselective and homoselective synthesis of aryl azides. *Appl. Organomet. Chem.* **2018**, *32* (9), No. e4436.
(52) Haghshenas Kashani, S.; Landarani-Isfahani, A.; Moghadam, M.; Tangestaninejad, S.; Mirkhani, V.; Mohammadpoor-Baltork, I. Nano−silica functionalized with thiol−based dendrimer as a host for gold nanoparticles: An efficient and reusable catalyst for chemoselective oxidation of alcohols. *Appl. Organomet. Chem.* **2018**, *32* (9), No. e4440.
(53) Rahman, T.; Borah, G.; Gogoi, P. K. Activated Mont K10-Carbon supported Fe 2 O 3: A versatile catalyst for hydration of nitriles to amides and reduction of nitro compounds to amines in aqueous media. *J. Chem. Sci.* **2021**, *133*, 1−12.
(54) Abdolahi, S.; Gholamian, F.; Hajjami, M. Preparation and catalytic application of two different nanocatalysts based on hexagonal mesoporous silica (HMS) in synthesis of tetrahydrobenzo[b]pyran and 1,4-dihydropyrano[2,3-c]pyrazole derivatives. *Sci. Rep.* **2022**, *12*, 22108−22139.
(55) Goto, A.; Endo, K.; Saito, S. Rh(I)-Catalyzed Hydration of Organonitriles under Ambient Conditions. *Angew. Chem., Int. Ed.* **2008**, *47* (19), 3607−3609.
(56) Kazemi Miraki, M.; Arefi, M.; Salamatmanesh, A.; Yazdani, E.; Heydari, A. Magnetic nanoparticle-supported Cu−NHC complex as an efficient and recoverable catalyst for nitrile hydration. *Catal. Lett.* **2018**, *148*, 3378−3388.
(57) Poeschl, A.; Mountford, D. M. A facile manganese dioxide mediated oxidation of primary benzylamines to benzamides. *Org. Biomol. Chem.* **2014**, *12* (36), 7150−7158.
(58) Timelthaler, D.; Schöfberger, W.; Topf, C. Selective and additive-free hydrogenation of nitroarenes mediated by a DMSO-tagged molecular cobalt corrole catalyst. *Eur. J. Org. Chem.* **2021**, *14*, 2114−2120.
(59) Yamanaka, N.; Hara, T.; Ichikuni, N.; Shimazu, S. Chemoselective hydrogenation of 4-nitrostyrene to 4-aminostyrene by highly efficient TiO_2 supported Ni3Sn2 alloy catalyst. *Bull. Chem. Soc. Jpn.* **2019**, *92* (4), 811−816.
(60) Pehlivan, L.; Métay, E.; Laval, S.; Dayoub, W.; Demonchaux, P.; Mignani, G.; Lemaire, M. Alternative method for the reduction of aromatic nitro to amine using TMDS-iron catalyst system. *Tetrahedron* **2011**, *67* (10), 1971−1976.

https://doi.org/10.1021/acsomega.4c08465
ACS Omega 2024, 9, 47811−47821